Inelastic Neutron Scattering Study of Water in Hydrated LTA-Type Zeolites

Carmelo Corsaro,[†] Vincenza Crupi,[†] Domenico Majolino,*[,†] Stewart F. Parker,[‡] Valentina Venuti,[†] and Ulderico Wanderlingh[†]

Dipartimento di Fisica, Università di Messina, C.da Papardo, S.ta Sperone 31, P.O. BOX 55, 98166 Messina, Italy and ISIS Facility, Rutherford Appleton Laboratory, Chilton, Didcot, OX11 QX, UK

Received: August 1, 2005; In Final Form: November 18, 2005

The vibrational dynamics of water molecules encapsulated in synthetic Na-A and Mg-exchanged A zeolites were studied versus temperature by inelastic neutron scattering (INS) measurements (30−1200 cm^{-1}) as a function of the induced ion-exchange percentage by using the indirect geometry tof spectrometer TOSCA at the ISIS pulse neutron facility (RAL, UK). The experimental INS spectra were compared with those of ice Ih to characterize the structural changes induced by confinement on the H_2O hydrogen-bonded network. We observed, after increasing the Mg^{2+} content, a tendency of water molecules to restore the bulklike arrangements together with more hindered dynamics. These results are confirmed by the analysis of the evaluated one-phonon amplitude-weighted proton vibrational density of states aimed, in particular, to follow the evolution of the water molecules librational mode region.

Introduction

Confinement in microporous materials is nowadays an attractive subject of a great variety of both experimental and theoretical studies.[1−4] The case of nanoconfined water is of particular importance because understanding how the various confining matrixes modify the water properties compared to those of the bulk state is of utmost significance to control and optimize a broad spectrum of industrial processes. In the past decade, great interest was focused on the study of water in zeolites.[5−9]

Zeolites are nanoporous crystalline aluminosilicates that can be built up by corner sharing of TO_4 tetrahedral units (T = Si, Al). Their nominal formula is written as $X^{n+}_{x/n}$ $[(AlO_2)_x(SiO_2)_y]^{-x}$. For every AlO_4 tetrahedron, the framework gains a charge of −1. This charge has to be balanced by the presence of additional extraframework cations $X^{+n}_{x/n}$ that sit inside the pores of the zeolite. These species are often ion exchangeable as they are small enough to move through the pore systems of the zeolites. The zeolitic framework is created by the progressive connections of two adjacent TO_4 units that share an oxygen atom, realizing T−O−T bridges. The great flexibility of the T−O−T angle from ∼100° to ∼180° gives rise to a wide variety of different zeolites. They are characterized by internal voids, channels, and/or cavities of well-defined size in the nanometer range, 4−13 Å, accessible through apertures of well-defined molecular dimensions.[10] Inside the zeolitic channels, the behavior of water molecules is the result of a balance between the interactions of H_2O molecules with their water neighbors and with the zeolitic framework and extraframework cations, always via hydrogen bonds or ion−dipole interactions, i.e., between host−guest and guest−guest interactions. The understanding of the main characteristics of these interactions is important for a variety of applications in synthesis and material science research.

An overall picture of the equilibrium geometry and dynamics of water in zeolites can be obtained by the investigation of (i) the OH stretching and HOH bending by IR absorption techniques, (ii) the librational modes, (iii) water−cation and hydrogen-bond stretch by incoherent inelastic neutron scattering (IINS), and (iv) the rotational and translational diffusion as seen by incoherent quasi elastic neutron scattering (IQENS).

Recently, we studied the effect of ion exchange on the O−H stretching and H−O−H bending intramolecular vibrations and on the diffusional dynamics of water in zeolites Lynde-type A (LTA, from here on referred to as zeolite A) by Fourier transform infrared absorbance (FTIR)[11,12] and by IQENS[8,13] measurements. The samples under investigation were fully hydrated Na-A and a variety of Mg-exchanged A zeolites with an increasing Mg^{2+} ion content. The analysis was performed as a function of temperature. From the complete data set, we showed that confinement into zeolitic cavities allows water to maintain the hydrogen-bond arrangements typical of the bulk state. In this sense, we attributed to the zeolitic surface a "structure-maker" role on physisorbed water. In addition, this role was shown to be particularly enhanced by the partial exchange of monovalent and bivalent ions. This was evident in the IR spectra by the observation, under confinement, of the tetrahedral connectivity typical of bulk water that progressively increased with increasing Mg^{2+} content. IQENS data, in addition, revealed a higher fraction of nondiffusing water molecules involved in a tetrahedral hydrogen-bonded network as a consequence of partial cation substitution.

Here, we use INS to study the vibrational behavior of water molecules adsorbed in Na-A and two Mg-exchanged A zeolites, namely Mg50-A (the last one obtained by the Na-A exchange, with 50% of the Mg^{2+} ions) and Mg86-A as a function of temperature. We remark that the observed modes, particularly the libration dynamics, are very sensitive to the local environments of water modified as a consequence of confinement. A tentative assignment of the various modes of water is performed in agreement with the existing literature on water structural arrangements in these kinds of zeolites and comparing the

* To whom correspondence should be adddressed. E-mail: majolino@unime.it. Phone: +39 090 6765237. Fax: +39 090 395004.
[†] Università di Messina.
[‡] Rutherford Appleton Laboratory.

10.1021/jp054253w CCC: $33.50
Published on Web 12/21/2005

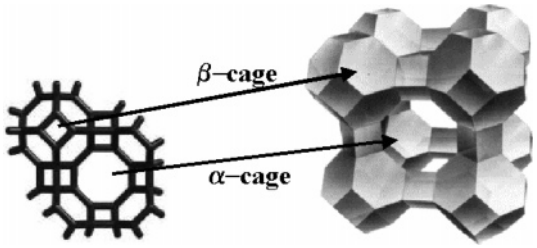

Figure 1. β-cage and α-cage that, gathered, give the typical LTA framework.

experimental INS spectra of zeolites with those of hexagonal ice Ih. The observed differences have been justified in terms of a balance among host−host and host−guest interactions and of the different number, position, and electronegativity of Na^+ and Mg^{2+} ions.

Finally, a detailed study of the one-phonon amplitude-weighted proton vibrational density of states (VDOS), $Z(\omega)$, is performed mainly to characterize the effects, induced by cation substitution and temperature, on the librational modes of interfacial water molecules.

Experimental Section

The INS measurements were obtained from synthetic $Na_{96}[Al_{96}Si_{96}O_{384}]\cdot 216H_2O$ (Na-A), $Mg_{24}Na_{48}[Al_{96}Si_{96}O_{384}]\cdot 249H_2O$ (Mg50-A), and $Mg_{41.3}Na_{13.4}[Al_{96}Si_{96}O_{384}]\cdot 266H_2O$ (Mg86-A). The samples were fully hydrated powders purchased from Nippon Chemical Industrial Co., Ltd. These formulas refer to the unit cell of fully hydrated materials, whose main properties can be found on the International Zeolites Association (IZA-SC) web site.[14] Figure 1 illustrates the cage-type framework of zeolite A. It is usually described as an octahedral array of sodalite units, called β-cages. These units, cubo-octrahedral in shape, consist of six four-membered rings separated by eight adjoining six-membered rings and have a free diameter of ∼6 Å. The interconnections of β-cages at the double four-membered rings give rise to larger α-cages with a free diameter of ∼10 Å. The A framework is constructed of α-cages by sharing the eight-membered rings, which are called windows and have a free diameter of ∼4.1 Å; thus, they can be penetrated by small molecules such as water.

The location of water molecules and their interactions with the zeolite A framework and extraframework cations have been widely studied both theoretically and experimentally. In the case of hydrated Na-A zeolite, the complete refinement of the pseudosymmetric structure has been achieved by using X-ray diffraction by Gramlich and Meier.[15] They quantitatively determined atomic coordinates, thermal parameters, interatomic distances, and bond angles. Higgins et al.[10] used atomistic simulation techniques to investigate the locations of water molecules in the framework of zeolite A and the effects of hydration on the location and stability of a range of extraframework mono- and bivalent cations. The main conclusions from the aforementioned studies are very useful for the interpretation of our spectra and will be discussed in detail in the Results and Discussion section.

INS spectra, at temperatures of 50, 180, and 220 K, were measured with the indirect geometry time-of-flight (tof) spectrometer TOSCA at the pulsed spallation neutron source ISIS (Rutherford Appleton Laboratory, Chilton, UK).[16] The data were collected over the range 24−4000 cm^{-1} (3−500 meV). The best results are normally obtained below 2000 cm^{-1} (250 meV). The resolution of the spectrometer is determined by a number of factors, but for practical purposes it can be taken to be 1.5% of the energy transfer. Instrumental resolution, combined with the high intensity of the ISIS source, allows for the study of the dynamics to high accuracy, reducing the background noise/signal ratio down to negligible for strongly scattering samples. In the current experiment, ∼3 g of powder for each zeolite sample was loaded into an aluminum sachet to give a sample thickness of ∼2 mm. This procedure was performed in a glovebox under an argon atmosphere. Cooling of the samples was achieved by mounting the aluminum sachet on a sample stick into a cryostat. For all of the analyzed temperatures, the spectra were accumulated over a period of 6 h. We observed that signals from the backscattering detectors bank showed lower noise levels than the forward-scattering bank; hence, we report here only INS spectra obtained from the backscattering detectors. The INS profiles were studied and interpreted only in the energy region from 30 to 1200 cm^{-1} (3−150 meV), because the highest energy-transfer part of the spectra (>1200 cm^{-1}) did not present significant features. The raw spectra were manipulated by using the standard procedures.[16] The bin size, i.e., the number of adjacent points averaged for each displayed data point, has been chosen to find the best compromise between accuracy and noise, and it was the same for all the samples investigated. As usual, the contribution from an empty can, resulting in a flat background, was subtracted from all of the INS spectra. The tof spectra were converted into $S(Q,\omega)$ versus energy loss spectra by using a standard ISIS data treatment program. The sample thickness used allowed us to obtain a scattering transmission from the sample that is greater or equal to 90%, so minimizing the multiple scattering contributions. We want to stress that on TOSCA, there exists a relation between energy and momentum transfer (Q, $Å^{-1}$) given by:

$$Q^2 = \frac{2m}{\hbar^2}(2E_f + \hbar\omega - 2\sqrt{E_f(E_f + \hbar\omega)}\cos\theta)$$

where the final energy $E_f \approx 4$ meV and the scattering angle $\theta = 135°$. Thus, each energy-transfer value is associated with a unique momentum transfer value, and the spectrometer takes a fixed trajectory (Q,ω) through space.

Our experimental data still contain multiphonon (MP) effects, which can only be minimized by lowering the temperature, a procedure which is not desirable if, as in our case, temperature effects are to be investigated. We evaluated the multiphonon contributions by an iterative procedure based on the assumption that the one-phonon term describes the INS spectrum at the lower-energy transfer and the subsequent calculation of the first MP term for the whole energy region from this first step. In this way, we obtained a new one-phonon spectrum that allows us to recalculate the MP terms in an iterative way until good convergence is achieved. This iterative procedure to correct the MP effects has been applied to all of the analyzed spectra. The density of states has been calculated after performing the MP and Debye−Waller factor corrections.

Figure 2 shows the INS spectrum of a Na-A sample at the highest investigated temperature, $T = 220$ K, as an example, together with the MP correction. As can be seen from an inspection of the figure, this correction only slightly affects the translational modes region at low frequency, but it increases at larger energy transfer.

Results and Discussion

As is well established,[17] the incoherent scattering cross section is much greater for hydrogen (80 barn) than any other element in the mineral (normally less than 5 barn), and it is also far greater than the coherent cross section of both hydrogen and the other elements. As a result, vibrations involving hydrogen

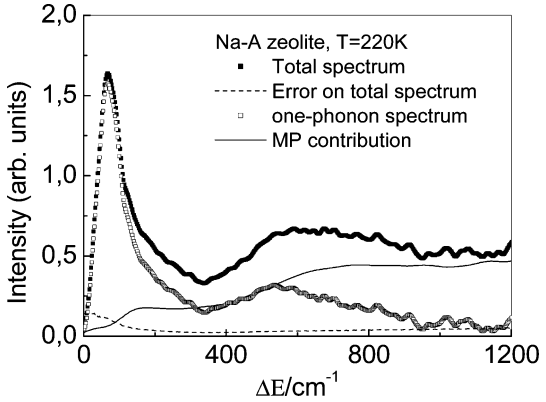

Figure 2. INS spectrum of Na-A zeolite at $T = 220$ K, together with the MP correction.

dominate the scattering spectrum. IINS is therefore an ideal tool for the study of water adsorbed in porous solids, with a negligible contribution coming from the inorganic framework of the host material. In particular, in the case of the Na-A zeolite framework, the coherent and incoherent cross sections turned out to be, respectively, $\sum_{coh} \approx 266.76$ barn and $\sum_{inch} \approx 19.61$ barn. For the Mg50-A zeolite framework, we obtained $\sum_{coh} \approx 267.6$ barn and $\sum_{inch} \approx 10.56$ barn. For the Mg86-A zeolite framework, we obtained $\sum_{coh} \approx 268.2$ barn and $\sum_{inch} \approx 3.29$ barn. The cross sections of the 27 H_2O molecules contained in the unit cell of Na-A zeolite were $\sum_{coh} \approx 209.25$ barn and $\sum_{inch} \approx 4314.6$ barn. The cross sections of the 31 H_2O molecules in the unit cell of Mg50-A zeolite resulted in $\sum_{coh} \approx 240.3$ barn and $\sum_{inch} \approx 4953.4$ barn. Finally, the cross sections of the 33 H_2O molecules in the unit cell of Mg86-A zeolite resulted in $\sum_{coh} \approx 255.8$ barn and $\sum_{inch} \approx 5273$ barn. The contributions to the total intensity coming from the zeolitic framework are mainly coherent and amount to 6% for Na-A, 5% for Mg50-A, and 5% for Mg86-A.

The intensity measured in the neutron scattering experiment corresponds to the incoherent double-differential cross section, which is given by

$$\left(\frac{d^2\sigma}{d\Omega dE}\right)_{\text{inc}} = \sum_d \frac{\sigma_d^{\text{inc}}}{4\pi} S_d^{\text{inc}}(,\omega) \qquad (1)$$

The sum on d is over the hydrogen atoms. The neutron momentum transfer, $\hbar\mathbf{Q}$, is defined by $\mathbf{Q} = \mathbf{k} - \mathbf{k}_0$, where $\mathbf{k}$ and $\mathbf{k}_0$ are the final and incident wave vectors, respectively. The INS spectrum is an energy-loss spectrum, because neutrons lose energy by exciting vibrational modes. Because nuclear interactions are not subject to dipole or polarizability selection rules, INS spectroscopy is sensitive to modes at all wavevectors across the Brillouin zone. This makes INS complementary to the infrared and Raman techniques, whose bands are observed at zero wavevector (Brillouin zone center). Thus, the incoherent scattering function, $S_d^{\text{inc}}(,\omega)$, can be calculated for fundamental transitions, for overtones, and for combinations. In general, the fundamental transitions will be the most-intense features of the spectra.

In Figure 3, the INS spectra are displayed for all of the analyzed samples at $T = 50$ K as an example. The error bars are approximately 5% in all of the figures.

Our spectra have been compared with the INS spectrum of ice Ih, as shown in Figure 4, reproduced here by permission from Dr. Ji-Chen Li.[18]

For our samples, all of the spectral range can be divided into two main regions, the first at lower energy, from 30 to 300

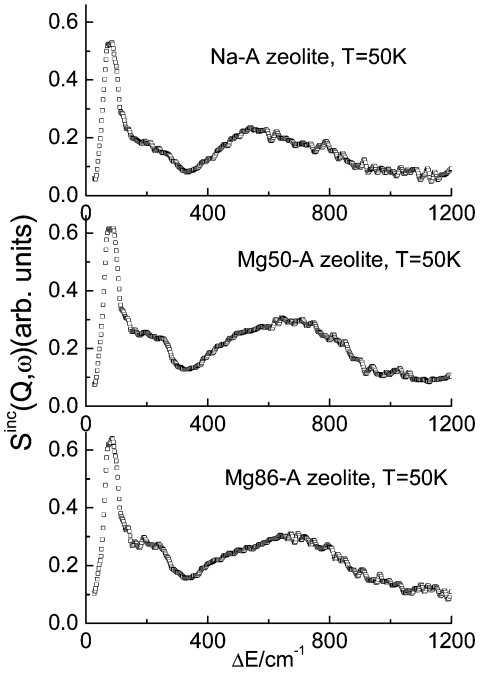

Figure 3. INS spectrum of Na-A, Mg50-A and Mg86-A zeolite at $T = 50$ K.

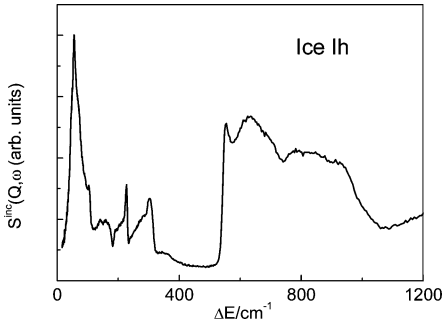

Figure 4. INS spectrum of ice Ih at $T = 27$ K.

cm^{-1}, in which cation−water stretch, intermolecular translational modes, and the hydrogen-bond stretch of water molecules are observable, and the second at higher frequency, from 300 to 1200 cm^{-1}, typical of intermolecular librational modes (rotational oscillations). We attempted to assign the various observed modes of water by taking into account the local environment of water in Na-A and in the Mg-exchanged A zeolites under investigation. Atomistic simulations techniques, employed by Higgins et al.,[10] showed in the case of Na-A zeolite that the preferred absorption site of the Na^+ cation is in the α-cage, in a six-ring window preferred site, 6-fold coordinated by four water molecules ($Na-O_w = 2.29$ and 2.41 Å) and two framework oxygen atoms ($Na-O_{fw} = 2.40$ and 2.42 Å). Three water molecules are located inside the α-cage and are stabilized by the interaction with the framework ($H\cdots O_{fw} = 2.17$ Å), whereas the fourth water molecule is located in the β-cage, perpendicular to the six-window where the sodium ion is located. The size of the channels appears to be "reduced" by the presence of cations in these positions, and this prevents the entrance of other molecules. The substitution of Na^+ ions with bivalent ions, such as Mg^{2+}, gives rise to a reduction of the number of ions in the zeolite. Furthermore, the energetically most-favorable adsorption sites for bivalent ions are calculated in the β-cage, in a six-membered ring, thus leaving the entrance channels to the zeolitic cavities free. In their adsorption site, bivalent cations are 4-fold-coordinated by four water molecules, arranged in tetrahedral coordination. On this basis, they reproduced the

experimental structure of a CaNa-A zeolite, a system analogous to our Mg-exchanged A zeolites. Water molecules, four per unit cell, turned out to be mainly located in the α-cage, near the eight-membered rings, and they form interactions with silicon and aluminum ions of the framework ($Si-O_w \approx 1.86$ Å, $Al-O_w \approx 2.00$ Å) framework oxygens ($H\cdots O_{fw} \approx 1.9$ and 1.85 Å) and extraframework Na^+ and Ca^{2+} cations ($Na-O_w \approx 2.6$ Å, $Ca-O_w \approx 2.4$ Å). With respect to the CaNa-A case, the differences expected for our Mg50-A and Mg86-A zeolites are related to the different ionic "force" of magnesium, which induces variations in the ion−dipole interactions with the adsorbate water.

On the basis of the above results, we can first hypothesize that the low-frequency band centered at ~80 cm^{-1}, which is a principal feature in all of the spectra, is the cation (Na or Mg)−water stretch. Only one water−cation stretch is observed, as expected, because each water molecule is attached to at least one cation. This band is also expected to reflect the translational modes of water molecules. The convolution of these modes could justify the wider peak with respect to that of ice Ih (at ~56 cm^{-1}). The crystal feature peaks observed at ~224 cm^{-1} and ~296 cm^{-1} for ice Ih in the high-energy part of the translational region, assigned to the hydrogen-bond stretch, do not completely disappear in the case of confined water in the zeolites but become much flatter and are merged into a large band. In particular, we notice that they can hardly be distinguished in the case of Na-A zeolite, whereas in passing to Mg-exchanged A zeolites with an increasing percentage of induced ion exchange, they appear progressively more pronounced, indicating the restoration of icelike crystal arrangements.

As far as the librational band is concerned, its lower energy, with respect to ice Ih, can be justified by taking into account that each water molecule is coordinated to at least one cation. Hence, the restoring force for the libration is relatively small. The hydrogen-bond interaction with the aluminosilicate framework oxygens and with the other water molecules is also expected to be relatively weak considering the rather large distances involved. We observe a low-frequency shift of the librational edge to ~306 cm^{-1} in the case of water in Na-A zeolite and to ~336 cm^{-1} in the case of water in Mg-exchanged A zeolites, with respect to the case of ice Ih in which it is observed at ~552 cm^{-1}, indicating a lowering of the librational force. A shift to a lower energy cutoff of the librational band, as well as the whole librational band itself, was also revealed with increasing pressure (and density) of ice existence on a $P-T$ phase diagram. X-ray and ND measurements indicated that for most ice phases, an increase of density corresponds to an increase of the nearest neighbor water−water distances.[19,20] Then, the softening of the transverse force constant between neighboring water molecules could be due to longer and weaker hydrogen bonds or, alternatively, that the water molecules in the small pores (~10 Å diameter) of zeolites exhibit deformed hydrogen bonds compared to bulk ice. This is in agreement with the structural results of water confined in different porous media such as Vycor or silica glasses, which show a strongly distorted hydrogen bond network even at room temperature,[21,22] and our previous FTIR measurements performed on water in Na-A and Mg-exchanged A zeolites (from 41 to 86% of cation substitution),[12] which indicated the existence of a bifurcated, distorted hydrogen bond (BHB) between three water molecules as a main feature of confined water. The position of the low-energy cutoff of the librational band tends to approach that of ice Ih on passing from Na-A to Mg50-A and Mg86-A zeolites. This result also indicates that, when the Mg^{2+} content is increased, confined water tends to exhibit hydrogen-bond arrangements closer to the bulk state. These last two observations can be explained by taking into account that with the reduction of the number of ions in the zeolitic voids as a consequence of cation substitution, the smaller ionic radii and the positioning of bivalent cations at the edge of the α-cages of the zeolitic framework effectively "increase" the size of zeolitic channels and, hence, favor a more regular formation of fully developed tetrahedral networks. In addition, on passing from Na-A to Mg50-A and Mg86-A samples, the librational band maximum moves toward higher energy from ~537 cm^{-1} for Na-A zeolite to ~640 cm^{-1} for Mg50-A zeolite and to ~693 cm^{-1} for Mg86-A zeolite, indicating an increased hindrance of the librational motion with an increasing percentage of induced ion exchange. This can be related to the restoring of icelike hydrogen-bonded networks, as already explained in terms of the reduced number of ions as a consequence of the cation substitution, together with the different positioning of bivalent cations. In fact, a reduced mobility of H_2O molecules confined in Mg50-A with respect to Na-A zeolites has already been shown as a consequence of the partial ion exchange by previous neutron-scattering measurements.[23] Our already cited FTIR measurements[12] showed a new class of H_2O molecules belonging to a network, tetrahedral in character, that involves four water molecules coordinated by the exchangeable cation, according to the simulation studies reported in the Experimental Section. These molecules exhibit hindered dynamics triggered by the extraframework cations in the confining matrix. In our case, this hindering is expected to be enhanced by the increased electronegativity of Mg^{2+} with respect to Na^+.

At this stage, we do not perform an analysis versus T of the measured spectra for each sample, because the influence of both the population factor and the Debye−Waller Factor (DWF) changes with temperature. To take them into account, the one-phonon vibrational density of states (VDOS, $Z(\omega)$) has been evaluated with the formalism of S. W. Lovesey[17] and is given by

$$Z(\omega) = \frac{2M\omega S^{\mathrm{inc}}(Q,\omega)}{Q^2\{1 + n(\omega)\}\exp\{-2W(Q)\}} \qquad (2)$$

where $n(\omega)$ is the Bose−Einstein factor defined by $\{\exp(\hbar\omega/k_BT) - 1\}^{-1}$, and the DWF is given by $2W(Q) = Q^2\langle u^2\rangle$, with $\langle u^2\rangle$ being the mean-square atomic displacement.

Figure 5 shows the evolution, as a function of T, of the one-phonon vibrational density of states for water confined in Na-A and Mg86-A zeolites as examples.

For both samples we observed, when the temperature is lowered, an upshift of the librational band from ~535 cm^{-1} at $T = 220$ K to ~563 cm^{-1} at $T = 50$ K for Na-A zeolite and from ~643 cm^{-1} at $T = 220$ K to ~687 cm^{-1} at $T = 50$ K for Mg86-A zeolite, reflecting an increasing hindrance of the librational motions, which reveals an amplified effect of confinement.

More detailed information has been obtained from fitting the librational band to a sum of Gaussian peaks. Three subbands have been used considering the three different librational modes of water molecules around its three symmetry axes: the x axis in the molecular plane, the y axis, which is the two-fold molecular symmetry axis, and the z axis perpendicular to the molecular plane (Figure 6, inset). On the basis of the existing literature,[24−26] the observed subbands ω_1, ω_2, and ω_3 correspond to the librational modes around the axes y, z, and x, respectively. Taking into account the structure of the zeolitic framework (···Si−O−Al···), we can hypothesize that the allowed librational modes for interfacial water molecules bound to the surface are the ones around the y and x axes (ω_1 and ω_3, respectively). On

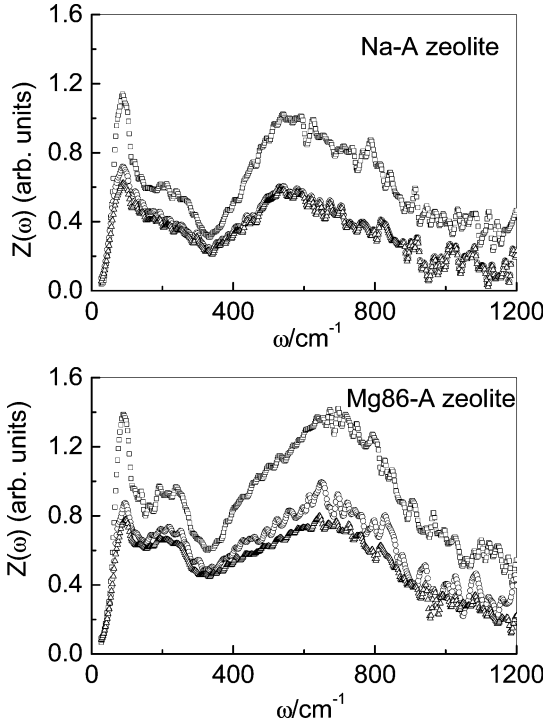

Figure 5. One phonon vibrational density of states for Na-A and Mg86-A zeolite at $T = 50$ K (□), $T = 180$ K (○) and $T = 220$ K (△).

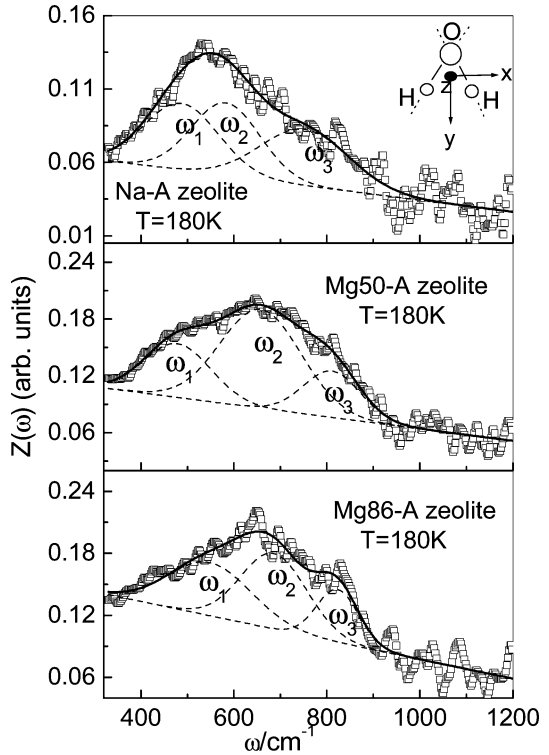

Figure 6. Librational band for Na-A, Mg50-A and Mg86-A zeolites at $T = 180$ K (□), together with the deconvoluted Gaussian components (dashed lines) corresponding to the three librational modes around the three symmetry axes of water molecules (see inset).

the other hand, all the librational modes are, in principle, allowed for H_2O molecules in the inner volume of the pore. Figure 6 shows the fitting results obtained for Na-A, Mg50-A, and Mg86-A zeolites at $T = 180$ K, as an example.

Figures 7 and 8 show the evolution of the librational band, as a function of temperature, for Na-A and Mg86-A zeolites, respectively, as an example.

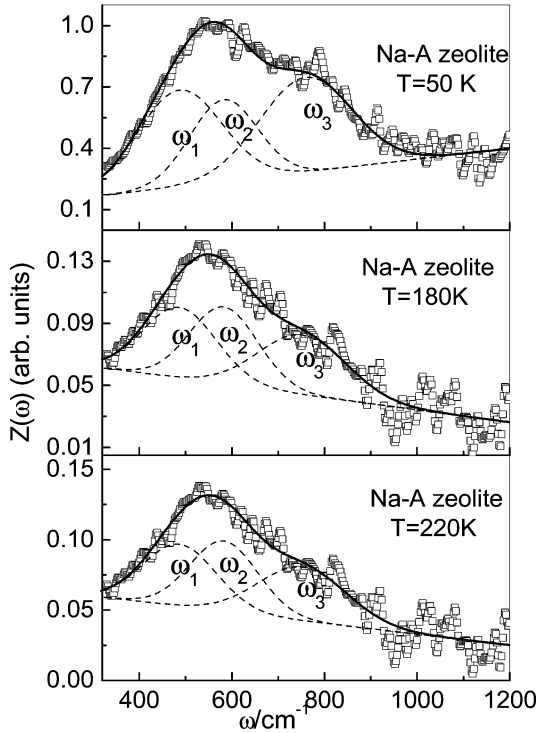

Figure 7. Librational band for Na-A zeolite (□) at $T = 50$, 180, and 220 K, together with the deconvoluted Gaussian components (dashed lines) corresponding to the three librational modes around the three symmetry axes of water molecules.

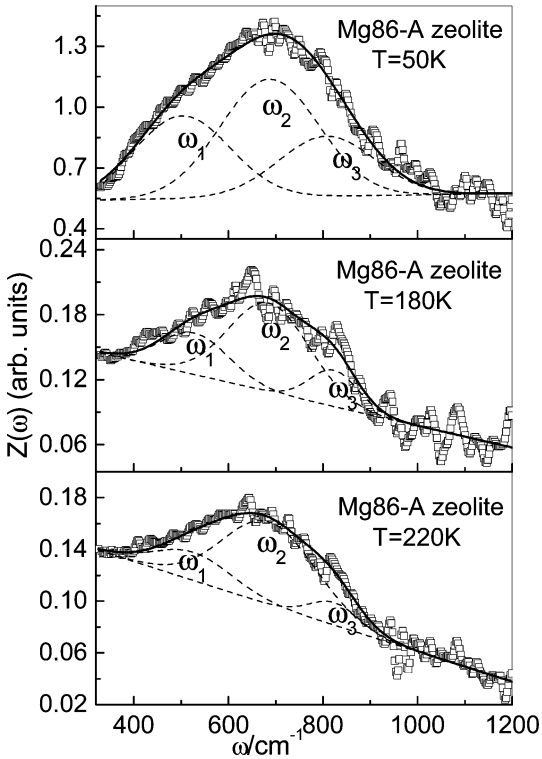

Figure 8. Librational band for Mg86-A zeolite (□) at $T = 50$, 180, and 220 K, together with the deconvoluted Gaussian components (dashed lines) corresponding to the three librational modes around the three symmetry axes of water molecules.

The main fitting parameters, i.e., center frequencies and percentage intensities, are reported in Table 1. All of the fitted curves reproduce the experimental data very well. Our best fit is characterized by a $r^2 \approx 0.9999$.

TABLE 1: Center Frequencies and Percentage Intensities of the Librational Bands as Obtained by the Best-Fit Procedure

T (K)	ω_1 (cm^{-1})	I_1 (%)	ω_2 (cm^{-1})	I_2 (%)	ω_3 (cm^{-1})	I_3 (%)
			Na-A Zeolite			
50	486.9	36.4	582.5	24.6	759.6	39.0
180	486.9	33.2	582.6	32.4	752.0	34.5
220	491.3	32.3	584.0	34.1	755.5	33.7
			Mg50-A Zeolite			
50	500.5	34.0	667.8	40.4	807.6	25.6
180	498.2	25.3	657.4	56.1	811.0	18.6
220	501.2	21.7	668.1	63.5	804.3	14.8
			Mg86-A Zeolite			
50	512.5	31.2	686.7	45.9	817.6	23.0
180	528.7	24.1	685.6	60.9	823.1	15.0
220	525.8	19.6	686.1	70.2	824.6	10.2

As far as the position of the librational subbands is concerned, it is well-known that it can be roughly correlated with the strength of the hydrogen bonding, because strong hydrogen bonding produces a strong restoring force and, hence, a high frequency. Taking this observation into account, we can relate the observed (see Table 1, Figure 6 as reference) high-frequency shift of the librational subbands passing from Na-A to, in order, Mg50-A and Mg86-A zeolites to a favored formation of a more extended tetrahedral hydrogen-bonded network with a stronger hydrogen bond because of the partial exchange of Na^+ with Mg^{2+} cations.

This favored formation of more stable icelike arrangements is confirmed also by the analysis of the amplitude of the Gaussian components. In fact, by increasing the Mg^{2+} content, we observe, as the main result at all of the investigated temperatures, an attenuation of the percentage intensities I_1 and I_3 of the librational modes ω_1 and ω_3, mainly connected with the hindered rotations of water bonded to the framework.

As far as the evolution in temperature is concerned (see Table 1 and Figures 7 and 8 as references), for each sample, no relevant changes have been observed in the obtained center frequencies and thus are not discussed here. The amplitude increase of the librational modes ω_1 and ω_3 as the temperature is lowered is a confirmation of the reduction of these degrees of freedom when the effects of confinement become more apparent.

Conclusions

In the present paper, we report an inelastic neutron scattering (INS) study, performed at different temperatures on water entrapped in synthetic A-type zeolites: Na-A and two different Mg-exchanged A-type zeolites, Mg50-A and Mg86-A, in which 50% and 86% of the monovalent cations Na^+ have been replaced with bivalent Mg^{2+}, respectively. The aim was to investigate the effect of the induced ion exchange on the structural arrangements of the confined H_2O molecules by an analysis of the wide vibrational range (30−1200 cm^{-1}) that can be covered with this technique.

For all of the investigated samples, the existence of a distorted hydrogen-bond network, as a consequence of confinement, has been revealed by the observed lower energy cutoff of the librational band with respect to ice Ih.

Furthermore, by increasing the Mg^{2+} content, we observed the appearance of crystal feature peaks in the high-energy translational region, typical of a hydrogen-bond stretch in ice Ih, together with the reduction (with respect to ice Ih) of the aforementioned low-frequency shift of the librational edge. These findings reveal that an increasing percentage of induced ion exchange can favor more "icelike" tetrahedral conformations of H_2O molecules.

For all of the analyzed samples, the evolution versus T of the proton density of states shows that the hindrance of the librational motion increases by lowering T, as revealed by a shift to higher frequency of the maximum of the librational band.

The deconvolution into a Gaussian profile of the experimental librational band revealed that as the Mg^{2+} content is increased, there is an attenuation of the librational modes connected to hindered rotations of water molecules attached to the zeolitic surface.

Acknowledgment. We thank Dr. D. Colognesi (CNR, 1st. Sistemi Complessi, Sesto Fiorentino, FI I-50019 Italy) for useful discussion during the data elaboration. The Rutherford Appleton Laboratory is thanked for access to neutron beam facilities.

References and Notes

(1) Klafter, J.; Blumem, A.; Drake, J. M. *Relaxation and Diffusion in Restricted Geometry*; Klafter J., Drake J. M., Eds.; New York: Wiley, 1989.

(2) Rupley J. A.; Careri, G. *Adv. Protein Chem*. **1991**, *41*, 37.

(3) Arndt, M.; Stannarius, R.; Gorbatschow, W.; Kremer, F. *Phys. Rev. E: Stat., Nonlinear, Soft Matter* **1996**, *54*, 5377.

(4) *Proceedings of the First International Workshop of Dynamics in Confinement;* Frick, B., Zorn, R., Buttner, H., Eds.; EDP Science: Les Ulis, France, 2000.

(5) Mizota, T.; Satake, N.; Fujiwara, K.; Nakayama, N. *Steam, Water and Hydrothermal Systems: Physics and Chemistry Meeting the Needs of Industry*, Proceedings of the 13th ICPWS; Tremaine, P. R., Hill, P. G., Irish, D. E., Balakrishnan, P. V., Eds.; NCR Research Press: Ottawa, Ontario, 2000.

(6) Beta, I. A.; Bohling, H.; Hunger, B. *PCCP* **2004**, *6*, 1975.

(7) Jobic, H.; Tuel, A.; Krossner, M.; Sauer, J. *J. Phys. Chem.* **1996**, *100*, 19545.

(8) Crupi, V.; Majolino, D.; Migliardo, P.; Venuti, V.; Wanderlingh, U.; Mizota, T.; Telling, M. *J. Phys. Chem. B* **2004**, *108*, 4314.

(9) Line, C. M. B.; Kearley, G. J. *J. Chem. Phys.* **2000**, *112*, 9058.

(10) Higgins, F. M.; de Leeuw, N. H.; Parker, S. C. *J. Mater. Chem.* **2002**, *12*, 124.

(11) Crupi, V.; Majolino, D.; Migliardo, P.; Venuti, V.; Mizota, T. *Mol. Phys.* **2004**, *102*, 1943.

(12) Crupi, V.; Longo, F.; Majolino, D.; Venuti, V. *J. Chem. Phys.* **2005**, *123*, 154072.

(13) Corsaro, C.; Crupi, V.; Majolino, D.; Migliardo, P.; Venuti, V.; Wanderlingh, U.; Mizota, T.; Telling, M. *Mol. Phys.* **2005**, accepted.

(14) Database of Zeolite Structure. http://www.iza-structure.org/databases/ (accessed Dec 2005).

(15) Gramlich, V.; Meier, W. M. *Z. Kristallogr*. **1971**, *133*, 134.

(16) Colognesi, D.; Celli, M.; Cilloco, F.; Newport, R. J.; Parker, S. F.; Rossi-Albertini, V.; Sacchetti, F.; Tomkinson, J.; Zoppi, M. *Appl. Phys. A: Mater. Sci. Process.* [Suppl.] **2002**, *74*, S64−S66; See also Mitchell, P.; Parker, S.; Ramirez-Cuesta A.; Tomkinson, J. *Vibrational Spectroscopy with Neutrons With Applications in Chemistry, Biology, Materials Science and Catalysis;* World Scientific Publishing Company: Hackensack, NJ, 2005.

(17) Lovesey, S. W. *Theory of Neutron Scattering from Condensed Matter*; Adair, R. K., Elliott R. J., Krumhansl, J. A., Marshall, W., Wilkinson, D. H., Eds.; Clarendon Press: Ottawa, Ontario, 1986.

(18) Li, J. *J. Chem. Phys.* **1996**, *105*, 6733.

(19) Kamb, B.; Hamilton, W. C.; LaPlace, S. J.; Prakash, A. *J. Chem. Phys.* **1971**, *55*, 1934.

(20) Kuhs, W. F.; Finney, J. L.; Vettier, C.; Bliss, D. V. *J. Chem. Phys.* **1984**, *81*, 3612.

(21) Bruni, F.; Ricci, M. A.; Soper, A. K. *J. Chem. Phys.* **1998**, *109*, 1478.

(22) Soper, A. K.; Bruni, F.; Ricci, M. A. *J. Chem. Phys.* **1998**, *109*, 1486.

(23) Corsaro, C.; Crupi, V.; Longo, F.; Majolino, D.; Venuti, V.; Wanderlingh, U. *Phys. Rev. E: Stat., Nonlinear, Soft Matter* **2005**, accepted.

(24) Rahman, A.; Stillinger, F. H. *J. Chem. Phys.* **1971**, *55*, 3336.

(25) Hall, P. G.; Pidduck, A.; Wright, C. J. *J. Colloid Interface Sci.* **1981**, *79*, 339.

(26) Crupi, V.; Majolino, D.; Migliardo, P.; Venuti, V. *J. Phys. Chem. B* **2002**, *106*, 10884.